CHAPTER 4

Spectrum Selectivity and Responsivity of ZnO Nanoparticles Coated Ag/ZnO CQDs/Ag Ultraviolet Photodetectors*

Contents

*Part of this work has been published as:

Yogesh Kumar et al. “Spectrum Selectivity and Responsivity of ZnO Nanoparticles Coated Ag/ZnO QDs/Ag UV Photodetectors”, *IEEE Photonics Technology Letters*, 30 (12), 1147-1150, 2018.

CHAPTER 4

Spectrum Selectivity and Responsivity of ZnO Nanoparticles Coated Ag/ZnO CQDs/Ag Ultraviolet Photodetectors

4.1 Introduction

The ZnO based photodetectors exhibit a broad spectral response covering UV-B to UV-A (Liu *et al.*, 2010; Chen *et al.*, 2015). Thus, ZnO based sensors are not spectrum selective in nature. In general, spectrum selectivity in photodetectors is achieved by mainly three types of techniques as discussed in Chapter-1: (i) by selecting the active material of the detector which has a narrow absorption range (Lin *et al.*, 2015), (ii) by using an additional filter with the photodetector (Yu and Tian, 2016a) and, (iii) by improving the response of the detector over a specified region by means of other effects such as the plasmonic effect (Fang *et al.*, 2015). Most of the researchers have used external optical filters to achieve narrowband spectrum selective nature in photodetectors but at the cost of reduced responsivity (Ni *et al.*, 2012; Shen *et al.*, 2013; Qiao *et al.*, 2016). However, Ni et al.(Ni *et al.*, 2012), Shen et al. (Shen *et al.*, 2013) and, Yu and Tian (Yu and Tian, 2016b) have used n-ZnO, p-ZnO, and ZnO NPs respectively as a filter layer in their detector structures for achieving the spectrum selectivity with improved responsivity. In Chapter 3, we have fabricated a spectrum selective ZnO QDs based UV photodetector with a FWHM of ~49 nm without using any kind of external optical filter. The narrow FWHM is achieved by using the quantum confinement effect of the ZnO QDs. We have also achieved a very high responsivity due to the back to back Schottky barrier between adjacent QDs which reduces the noise/dark current (Xu *et al.*, 2014). In this Chapter, we will use an additional ZnO NPs

based filtering cum scattering layer on the MSM photodetector structure considered in Chapter-3 to improve both the spectrum selectivity and responsivity of the device. The prepared device is then analyzed under UV illumination from the front and back side of the UV detector. The deposited ZnO NPs act as an optical filter layer from front side illumination while the same ZnO NPs layer act as a scattering layer under back illumination. The effects of the ZnO NPs based scattering/filter layer on the responsivity and spectrum selectivity are analyzed. The outline of this chapter can be given as follows:

Section 4.2 presents the experimental details such as synthesis of ZnO NPs and the fabrication procedure of the photodetector with ZnO NPs layer. Section 4.3 includes the results and discussion regarding the film morphology of ZnO NPs, scattering theory and electro-optical characteristics such as current-voltage, time response and photo responsivity under dark and UV illumination of the PDs.

4.2 Experimental Details

The section includes the fabrication process of the ZnO nanoparticle coated Ag/ZnO QD/Ag detector. The fabrication process of the photodetector is same as discussed in chapter 3. Here, we have added the ZnO NPs layer on the top side of the detector as fabricated in chapter 3. The ZnO NPs layer acts as a filter and scattering layer under the UV illumination from front side and back side of the photodetector.

4.2.1 Preparation of ZnO QDs and ZnO NPs

The synthesis of ZnO QDs is performed by dissolving zinc acetate dehydrate as a precursor in 2-methoxyethanol under the steady state flow of the nitrogen gas in the three-neck flask as described in chapter 2. The prepared solution is filtered using PVDF

membrane (0.22 μm) to filter out the unreacted particles from the solution for enhancing the surface uniformity.

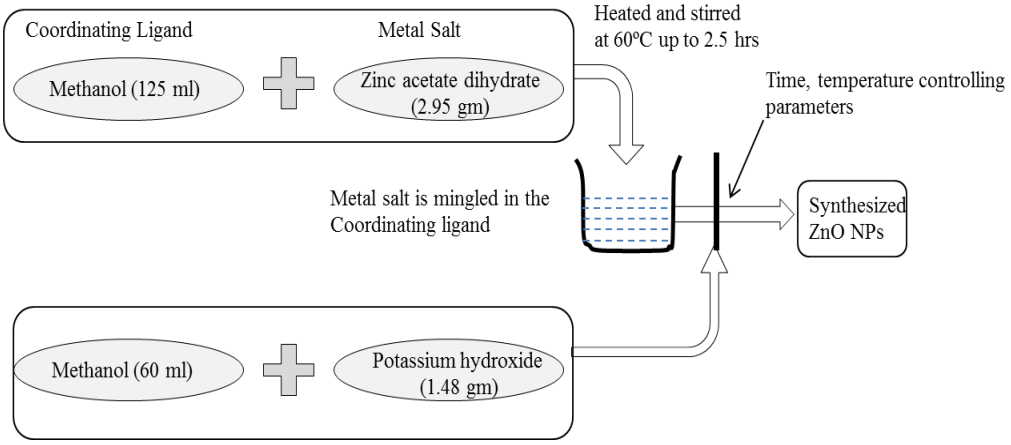

Figure 4. 1: ZnO NPs synthesis process

The ZnO NPs were synthesized by dissolving the zinc acetate dehydrate (2.95 gm) in the 125 ml of methanol solution and then placing at 60-65ºC temperature with continuous stirring. Meanwhile, the solution of potassium hydroxide KOH (1.48 gm) is also prepared in 60 ml of methanol ultrasonically for 5 min. The prepared KOH solution was added slowly into the zinc acetate solution and is kept stirring continuously for 2.5 hrs (Chuang *et al.*, 2014). The complete synthesis processed is shown in Figure 4. 1. The prepared solution looks like a milky white in color. Finally, the solution was centrifuged at 5000 rpm for 5 min and is then washed with methanol. Further, the prepared NPs are dissolved in 10 mg/ml of chloroform as a final solution.

4.2.2 Fabrication of Photodetector

In this work, we have followed the same device fabrication process that has already mentioned in chapter 3. The interdigitated Ag thin film (of thickness ~80 nm) electrodes are used for the channel length of 300 μm and channel width of 5 mm of the device as shown in Figure 4. 2. After electrode deposition, ZnO NPs was deposited on the top of

the electrodes and dried at room temperature. Figure 4. 2 illustrates the schematic device structure with the thicknesses ~100 nm and ~500 nm of ZnO QDs active layer and ZnO NPs filter and scattering layer respectively. The complete fabrication process as shown in Figure 4. 3.

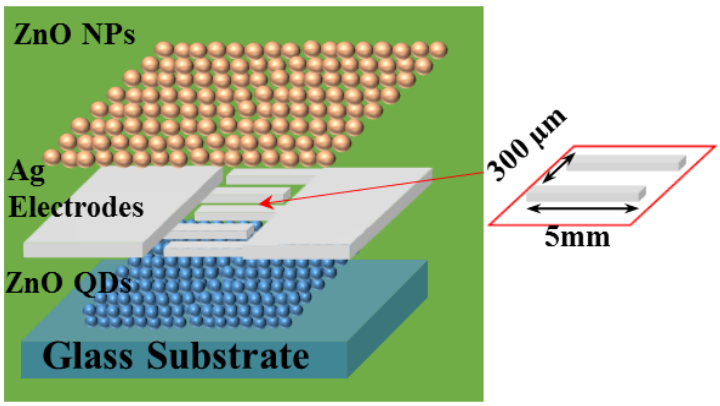

Figure 4. 2: Device structure fabricated on glass substrate with interdigitated Ag electrodes spacing 300µm.

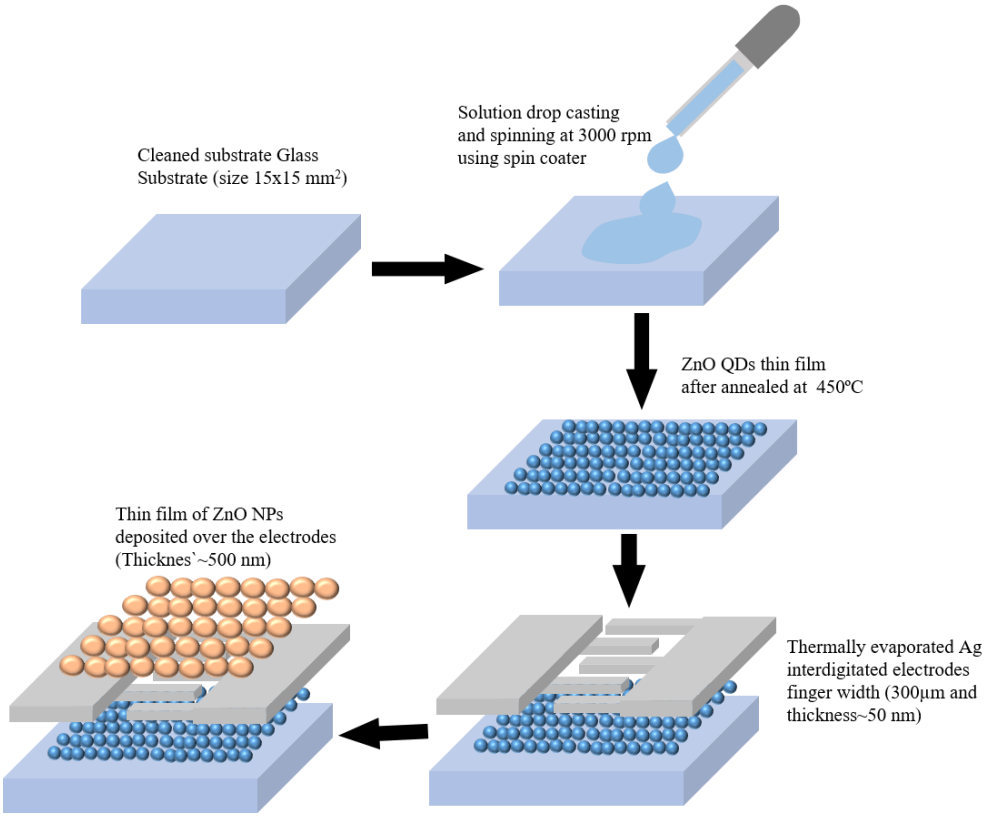

Figure 4. 3: Device fabrication flow of process.

4.3 Result and Discussion

4.3.1 Structural Characterization of ZnO NPs

The surface morphology and selected area electron diffraction (SAED) pattern of the as-grown ZnO QDs and HRSEM of annealed ZnO QDs have already been discussed in chapter 2. The XRD pattern of the ZnO QDs thin film annealed at 450 ºC also discussed in chapter 2.

The average particle size of ~300 nm of the ZnO NPs is confirmed from the SEM image shown in Figure 4. 4 (a). The size of the ZnO NPs are eligible for scattering of light as given by Mie Scattering theory (Zhang *et al.*, 2012). The XRD of the ZnO NPs shown in Figure 4. 4 (b) confirms the wurtzite type polycrystalline behavior of the film.

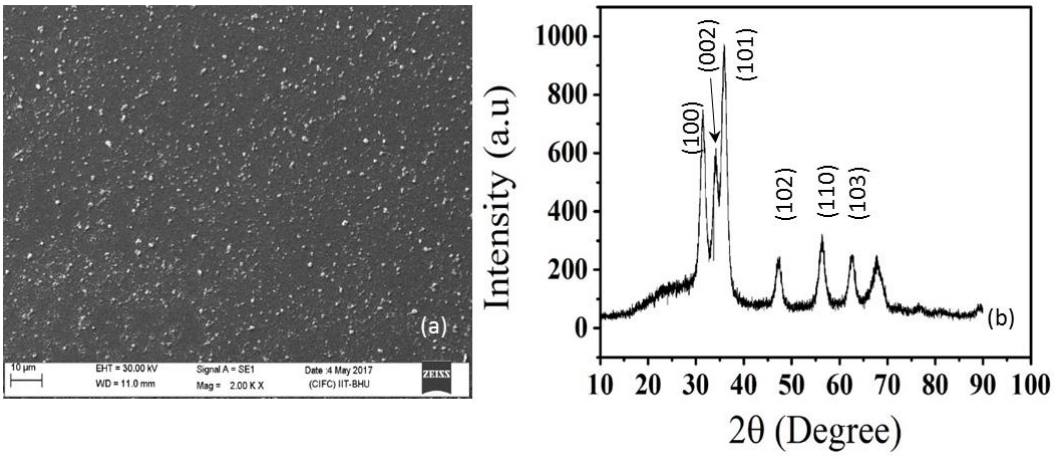

Figure 4. 4: (a) SEM image of ZnO NPs, and (b) XRD pattern of ZnO NPs.

4.3.2 Scattering Analysis of ZnO NPs

The phenomenon where the light is propagated in the presence of small physical object known as the scattering in optics. The laws of reflection and refraction defined, when light is incident on object, the radiation may either propagate in the forward direction, giving rise to refraction and absorption, or propagate in the backward direction, causing reflection, as shown in Figure 4. 5. However, under certain condition

when the dimensions of the object are on the order of the wavelength of light, the radiation will be spread in all directions that deviate. Such an optical phenomenon is called light scattering, and the object that causes the light scattering is known as the scatterer or scattering center.

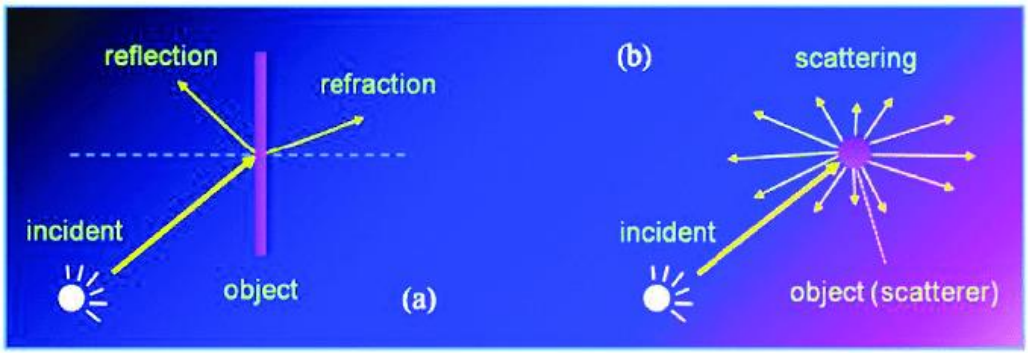

Figure 4. 5: reflection, refraction, and scattering of light (Zhang et al., 2012).

The scattering is inherent phenomenon of the nanoparticles in spherical dimension. It has been described by Rayleigh scattering theory and Mie scattering theory. Theory of the Rayleigh scattering determines the dielectric (non-absorbing) scatterers with a small size. In another case where the scattering system consists of large particles, i.e. the size (r) of the particles is comparable to the wavelength (λ) of the incident light, and the refractive index of the particle (m), Mie scattering theory is the only theoretical description is applicable. The Mie scattering theory can be calculated in terms of scattering factor (σ_{scat}) and scattering efficiency (Q_{scat}) as given:

$$\sigma_{scat} = \frac{\lambda^2}{2\pi} \sum_{n=0}^{\infty} (2n+1) \left(|a_n|^2 + |b_n|^2 \right) \tag{4.1}$$

Where the parameters a_n and b_n defined by the Riccati Bessel function ψ and ξ as

$$a_n = \frac{\psi_n(\alpha)\psi_n'(m\alpha) - m\psi_n(m\alpha)\psi_n'(\alpha)}{\xi_n(\alpha)\psi_n'(m\alpha) - m\psi_n(m\alpha)\xi_n'(\alpha)} \tag{4.2}$$

$$b_n = \frac{m\psi_n(\alpha)\psi_n'(m\alpha) - \psi_n(m\alpha)\psi_n'(\alpha)}{m\xi_n(\alpha)\psi_n'(m\alpha) - \psi_n(m\alpha)\xi_n'(\alpha)} \tag{4.3}$$

Where, $\alpha = 2\pi \times r / \lambda$, and the Riccati Bessel function can be defined as,

$$\psi_n(x) = \sqrt{\frac{\pi x}{2}} J_{n+\frac{1}{2}}(x) \tag{4.4}$$

$$\xi_n(x) = \sqrt{\frac{\pi x}{2}} \left[J_{n+\frac{1}{2}}(x) + iY_{n+\frac{1}{2}}(x) \right] \tag{4.5}$$

and the derivatives of the Riccati Bessel function can be defined as,

$$\psi_n'(x) = \psi_{n-1}(x) - \frac{n}{x}\psi_n(x) \tag{4.6}$$

$$\xi_n'(x) = \xi_{n-1}(x) - \frac{n}{x}\xi_n(x) \tag{4.7}$$

The scattering efficiency according to Mie scattering theory can be calculated as

$$Q_{scat} = \frac{\sigma_{scat}}{\pi \times r^2} \tag{4.8}$$

The above calculation of the scattering efficiency vs wavelength plotted for a fixed diameter of the particle size 300 nm as shown in Figure 4.6 exhibits the light scattering is occurred mainly from the 300 nm to 600 nm wavelengths.

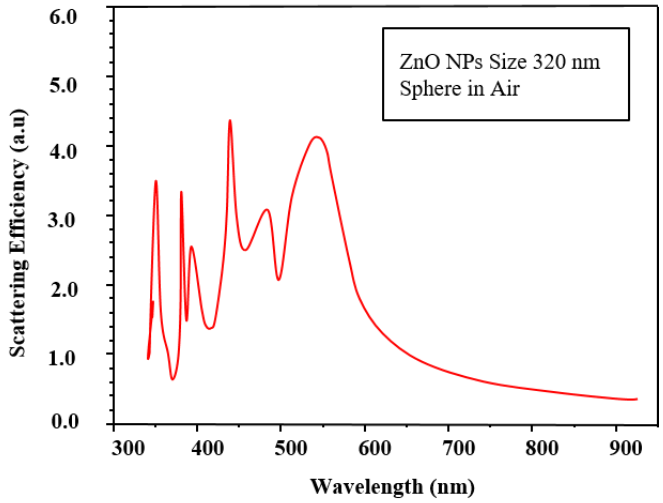

Figure 4. 6: Scattering efficiency dependence on the particle size and incident wavelength

4.3.3 Optical Characterization

Figure 4. 7 shows the absorption and transmittance characteristics of the layers ZnO QDs and ZnO NPs respectively. The transmittance of ZnO NPs reaches 10% to 80% within 350-375 nm. The photons with wavelengths larger than ~350 nm can easily pass through the ZnO NPs layer while the photons with wavelengths smaller than about ~390 nm can be absorbed in the active ZnO QDs to result in the photocurrent in the device. Clearly, the ZnO NPs layer acts as filter layer to result in an effective absorption of light in the active ZnO QDs over a very narrow wavelength region of 350 nm - 375 nm as demonstrated by the shaded region in Figure 4. 7.

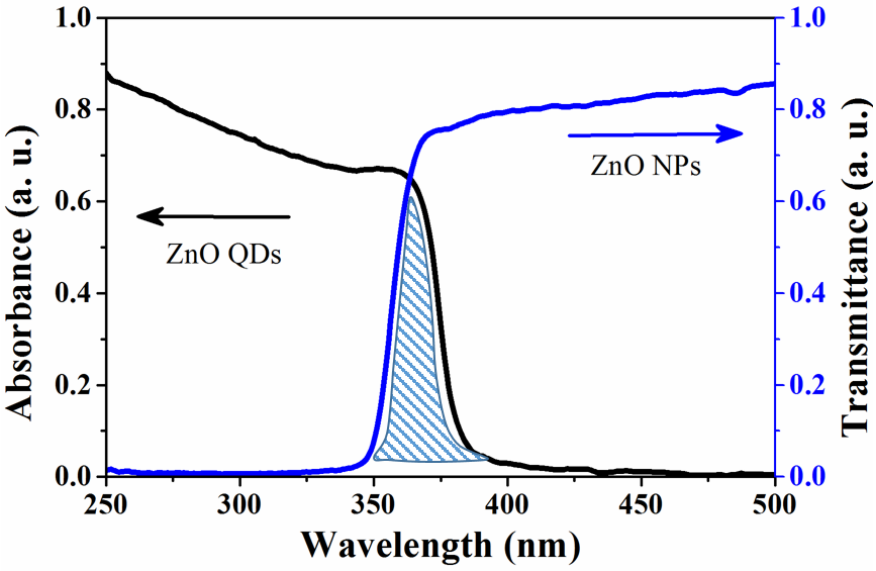

Figure 4. 7: Absorbance spectrum of ZnO QDs (film thickness ~100nm) deposited on quartz substrate and Transmittance of ZnO NPs (film thickness ~500nm).

4.3.4 Electro-Optical Characterization

The section has described the electrical characteristics of the photodetector an applied bias 0 to 10 V under the dark and UV illumination. The electro-optical characteristics: responsivity vs wavelengths and time response are measured under the dark and UV illumination also discussed in this section.

4.3.4.1 Current Voltage Characterization

The current density-voltage (J-V) characteristics of the fabricated photodetectors measured by the semiconductor parameter analyzer (KeySight, B1500A) are shown in Figure 4. 8. The J-V characteristics of the photodetector reported in chapter 3 are compared with those of our present Ag/ZnO QDs/Ag device coated with ZnO NPs. The measurement is performed under the dark condition with voltage swipe from 0 to 10 V. The J-V characteristics under dark condition clearly shows that the ZnO NPs layer has a negligible effect on the charge transport between the Ag electrodes and the ZnO QDs layer used as the active layer in the device.

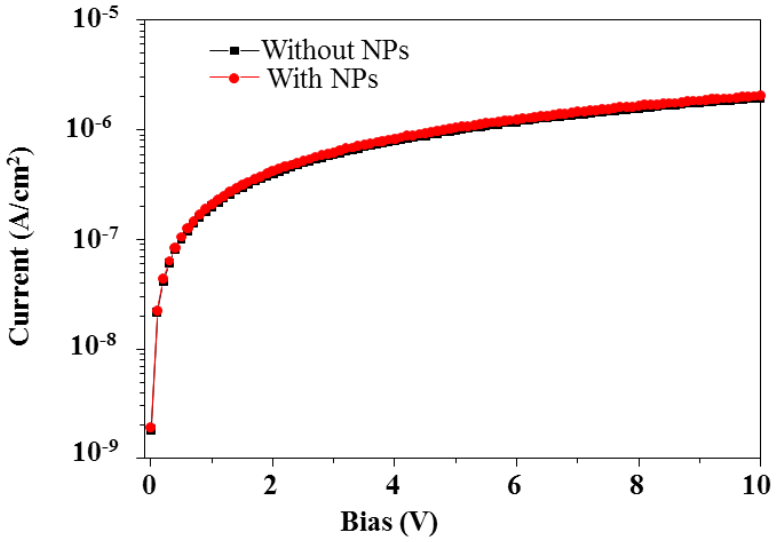

Figure 4. 8: Dark current density Vs voltage characteristics of Ag/ZnO-QD/Ag and ZnO NPs coated Ag/ZnO-QDs/Ag photodetector.

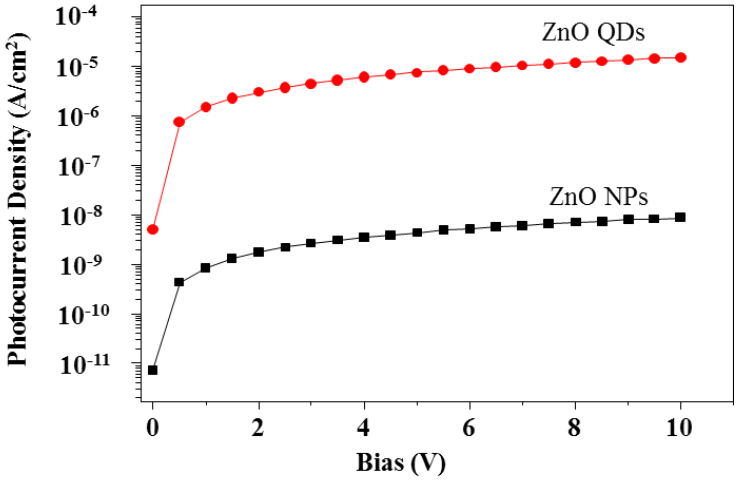

Figure 4. 9: J-V characteristics of ZnO NPs and ZnO QDs separately acts as active layer under the UV illumination of power density (~70 µW/cm2) at an wavelength 360 nm.

Figure 4. 9 compares the photoresponse of the separately fabricated Ag/ZnO NPs/Ag and Ag/ZnO CQDs/Ag devices. The nearly negligible response of the ZnO NPs active layer based device as compared to that of the ZnO QDs active layer based MSM device, which is confirms that ZnO QDs layer acts as an active layer while the ZnO NPs layer acts as a filter and scattering layer in our proposed MSM device. The effect of the

ZnO NPs on the photoresponse of the device under front and back illuminations can be described in the next section.

4.3.4.2 Responsivity Characterization

The responsivity (R_e) of the photodetector has been calculated as disussed in earlier chapters: The responsivity has been measured using a monochromator (SP2150i, Princeton Instruments) set up along with a digital multimeter (Agilent, 34410A) and power meter (PM100D, Thorlabs) as measured in chapter 2 and chapter 3. The peak responsivity of the photodetector measured under the front and back illuminations are ~6 A/W and ~20 A/W at a fixed applied bias of 2 V between the wavelength 350-375 nm respectively.

Photoresponse under Front Illumination: In this case, the device under study is illuminated from the front side so that light can enter into the active ZnO QDs layer through ZnO NPs deposited on the Ag electrodes as shown in Figure 4. 10 (a). It has been reported that most of the scattered light travels in the opposite direction to that of the incident light (Zhou *et al.*, 2014). Thus, a large fraction of the incident light is lost due to reflection, absorption, and scattering of the ZnO NPs layer under the front illumination. The entered light into the active layer is further reduced by the filtering action of the NPs layer as discussed in Figure 4. 7. In brief, the light from 350 nm – 375 nm wavelengths with received intensity much smaller than that of the incident light on the NPs layer is finally entered to the active layer for contributing to the photocurrent of the device. As a consequence, both the photoresponse and spectral width of the MSM photodetector with ZnO NPs scattering layer under study are drastically reduced as compared to those of the device without the ZnO NPs layer under front illumination as shown in Figure 4. 10 (b). The comparison of the photoresponse of the device with and

without the ZnO NPs layer in Figure 4. 10 (b) clearly demonstrates that the reflection, scattering, absorption and filtering actions of the ZnO NPs layer result in the improved spectrum selectivity (with FWHM ~ 25 nm) at the cost of reduced photoresponse as compared to the device without the ZnO NPs layer.

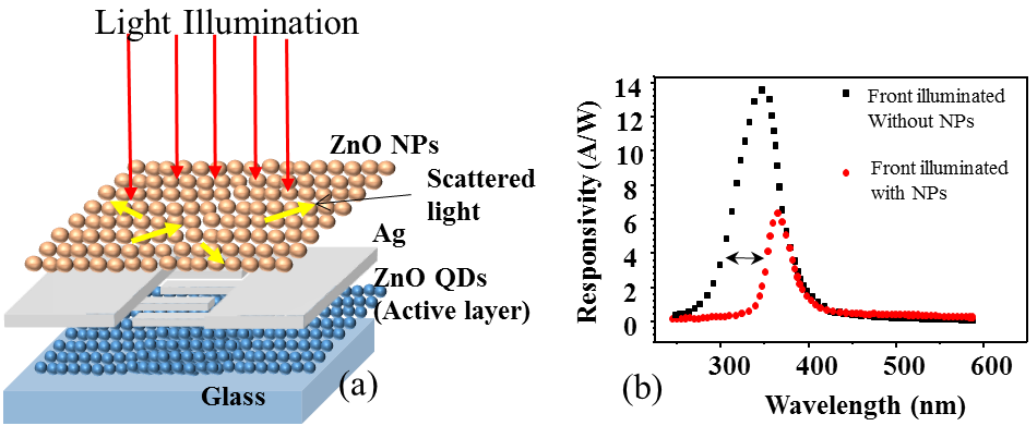

Figure 4. 10: Photoresponse under front illumination: (a) ZnO NPs acts as filter layer, and (b) spectral response (responsivity) of device.

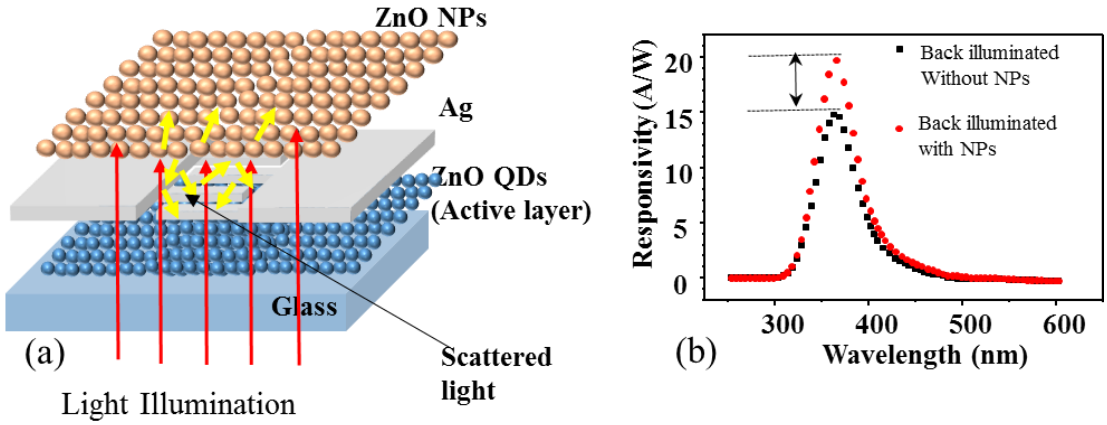

Figure 4. 11: Photoresponse under back illumination: (a) ZnO NPs acts as scattering layer, and (b) spectral response (responsivity) of the device.

Photoresponse under Back Illumination: In this case, light is entered into the device through the glass substrate as illustrated in Figure 4. 11 (a). The photoresponse under back illumination are compared for devices with and without ZnO NPs layer in

Figure 4. 11 (b). The photoresponse is observed to be larger in the device with NPs layer than that of the device without the NPs layer.

The increase in the responsivity can be atributed to two phenomenons:

(i) A part of the light is absorbed first in the ZnO QDs active layer and the remaining light then enters into the ZnO NPs based scattering layer. After absorption in the active layer, some part of the light transmitted through the active layer and entered into the ZnO NPs layer is scattered back in the opposite direction of the incident light (similarly as demonstrated by Zhou et al. (Zhou *et al.*, 2014) and enters into the active layer to re-absorption. This process enhances the resultant absorption in the ZnO QDs active layer thereby improving the responsivity of the device under back illumination as shown in Figure 4. 11 (b).

(ii) Since the incident light is first passed through the ZnO QDs layer, no filter action due to the ZnO NPs can take place in this case. Thus, the photons with wavelengths below ~390 nm are allowed to be absorbed in the active layer as per the absorption characteristics shown in Figure 4. 7. However, the photons with wavelengths above ~300 nm are attenuated and filtered out by the glass substrate to result in a spectrum selectivity of ~49 nm under back illuminated of the device reported in chapter 2 without the ZnO NPs layer.

The thin layer of ZnO NPs of ~300 nm considered in our study acts as a scattering layer for the photons entering into it after passing through the ZnO QDs layer. As a result, a fraction of the light incident on the ZnO NPs layer is fed back into the ZnO QDs active layer. The scattered photons from the NPs layer enhances the absorption in the ZnO QDs active layer thereby increasing the responsivity (see Figure 4. 11 (b)) of

the photodetector under study as compared to the device without the ZnO NPs layer reported in chapter 3. It may be mentioned that the enhanced responsivity under back illumination in present work agrees with the mechanism reported by (Hore *et al.*, 2006; Zhang *et al.*, 2012; Zhou *et al.*, 2014).

4.3.4.3 Time Response Characterization

The recoverable transient response is an important characteristic to identify the stability of the photodetector. It also gives information about the response speed of the device. It is measured under the illumination of the UV LED source (central frequency at 390 nm with an illumination density of 3.5 mW/cm^2) and a 2 V applied bias as shown in Figure 4.12 under front illumination and Figure 4.13 under back illumination. The UV LED generates the UV pulses and its switching controlled by an in-house designed Arduino microcontroller. The various parameters of our reported work as compared to other related works has been summarized in table 4.1.

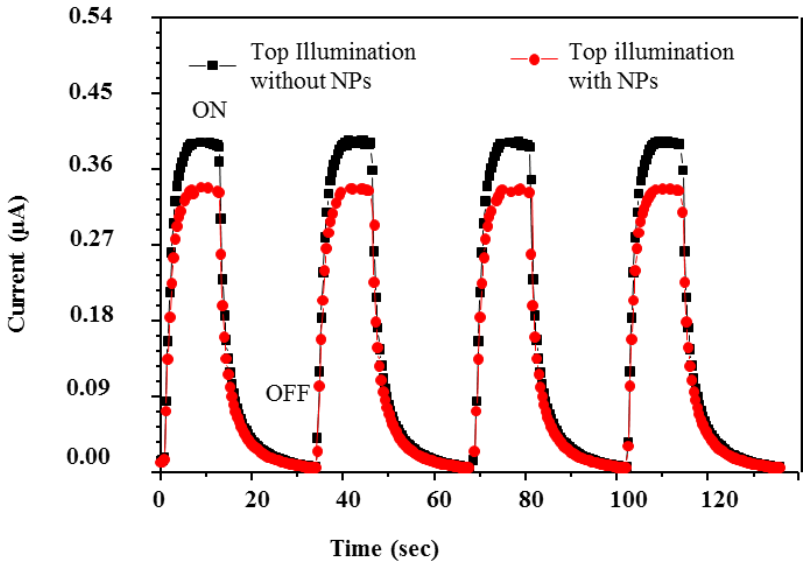

Figure 4.12: Filter effects on the time response under the illumination of UV LED from front side.

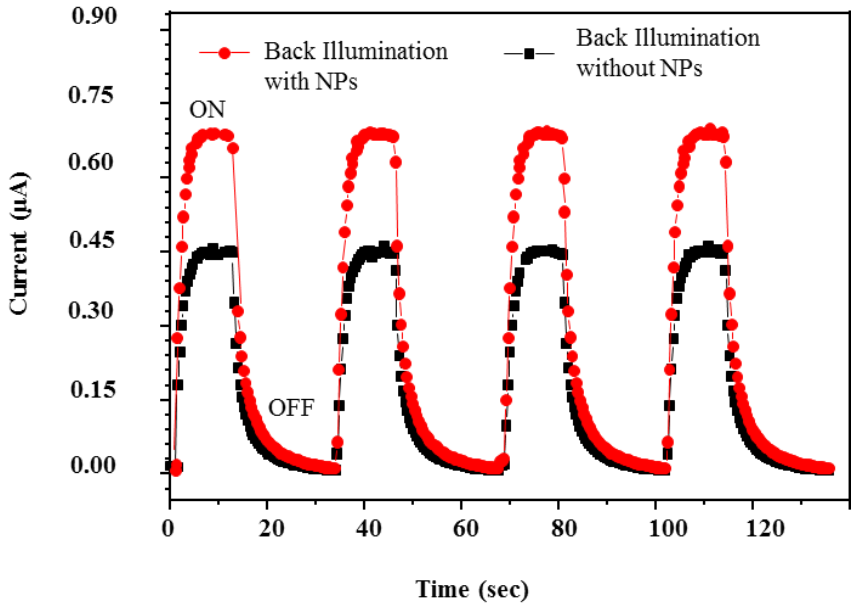

Figure 4.13: Scattering effects under the illumination of UV LED from back side of device with and without ZnO NPs.

Table 4.1: Comparison of Responsivity and FWHM of the NPs coated Ag/ZnO-QDs/Ag based photodetector with other similar work

Device structure	**Filter layer**	**Scattering layer**	**Peak Responsivity (A/W)**	**Applied bias (V)**	**FWHM (nm)**	**References**
Ag/ZnO/Ag	ZnO NPs	-	6	2	**25**	This work
Ag/ZnO/Ag	-	ZnO NPs	**20**	2	49	This work
i-ZnO/n-ZnO	n-ZnO	-	30 µ	0	9	(Ni *et al.*, 2012)
p-ZnO:(Li,N)/n-ZnO	p-ZnO:(Li,N)	-	18 µ	0	9	(Shen *et al.*, 2013)
Au/ZnO/Au	ZnO NPs	ZnO NPs	0.052	3	10	(Yu and Tian, 2016b)
Au/PEDOT:PSS/PVK/ITO	(PVK and ITO)	-	0.11	-5	26	(Wang *et al.*, 2010)

4.4 Conclusion

In this chapter, we have demonstrated the filter and scattering effects of the ZnO NPs on the responsivity of the Ag/ZnO QD/Ag photodetector under front and back illuminations respectively. The ZnO NPs layer acting as a filter layer under front illumination provides the FWHM of ~25 nm with the responsivity of ~6 A/W while NPs layer acting as a scattering layer under back illumination gives the responsivity ~20 A/W with a FWHM of ~49 nm at an applied bias of 2 V. Thus, the use of a ZnO NPs layer in the photodetectors can provide an option for improving either the spectrum selectivity or the responsivity of the detector by operating the device under front or back illumination as discussed above. The proposed photodetector exhibits moderate rise time of 3.5 sec and decay time of 6.3 sec at an applied bias of 2 V. The detection properties of the photodetector are found to be stable and reproducible under both the front and back UV illuminations.